

Electronic theory for solid-solution hardening and softening of dilute Al-based alloys: Elastic-moduli enhancement of Al-Li alloys

Kin-ichi Masuda-Jindo

Department of Materials Science and Engineering, Tokyo Institute of Technology, Nagatsuda, Midori-ku, Yokohama 227, Japan

Kiyoyuki Terakura*

Institute for Solid State Physics, University of Tokyo, Roppongi, Minato-ku, Tokyo 106, Japan

(Received 22 August 1988; revised manuscript received 27 October 1988)

We discuss the characteristic solid-solution hardening and softening of Al-based fcc alloys using *ab initio* Korringa-Kohn-Rostoker augmented-spherical-wave electronic structure calculations. We choose the dilute Al- X alloy systems, X being Li, Be, Na, Mg, Ca, and Cu, which exhibit characteristic solid-solution hardening or softening; solute elements such as Li and Be significantly enhance the elastic moduli of Al-based alloys, while Mg and Ca decrease them strongly. On the other hand, a solute element like Cu has little effect on the elastic moduli. We will show that the characteristic solid-solution hardening or softening can be predicted correctly by total-energy calculations, and that they are correlated to the change in the lattice constants due to the solute atoms. Particular attention will be focused on the puzzling problem of solid-solution hardening of Al-Li alloys.

I. INTRODUCTION

The Al-based fcc alloys are very important for technological purposes. So far a number of Al-based alloys have been developed and utilized widely:¹ typical examples are Al-based alloys including Cu, Mg, Si, Zn, and Mn solute elements (known as duralmin or super duralmin). Furthermore, it has recently been recognized that Al-Li (Al-based fcc) alloys are particularly useful and potential candidates for aerospace materials because of their superior strength-to-weight ratio. In general, the strength of these materials is enforced by solid-solution hardening and/or precipitation hardening.²⁻⁵ However, the detailed strengthening mechanism of the alloys has not been elucidated theoretically.

Li has the atomic number 3 and the melting point of the bcc metal phase is 179°C. Young's modulus Y of the Li metal is only about 5–10 GPa,^{6,7} and this value is 1 order of magnitude smaller than that of Al, i.e., about 66 GPa.^{3,4,8} In view of these experimental data it is quite surprising that the solute element, Li causes a drastic increase of Young's modulus of Al-based alloys:⁸ the strengthening rate is higher than that for Be or Cu solutes. On the other hand, it is known that solute elements like Mg and Ca having much larger atomic numbers, 12 and 20, and higher Young's modulus than Li lead to a significant reduction of the elastic modulus of Al-based alloys. In Fig. 1 we summarize the experimental data on Young's moduli of Al-based alloys.^{3,7-10} It can be seen that Young's moduli of Al-based alloys depend quite sensitively on the species of the solute elements. It is the purpose of the present paper to clarify the mechanism of the solid-solution hardening or softening of Al-based fcc alloys using the first-principles band-structure calculations for the Al-based ordered compounds, Al_7X and Al_3X , with X denoting a solute ele-

ment.

In the present paper we restrict ourselves to the calculation of the bulk modulus of Al-based alloys, since the theoretical scheme is not well suited for Young's modulus or shear modulus calculations, in which the elastic deformation modes of nonhydrostatic components should be taken into account. Fortunately, however, Young's modulus is proportional to the bulk modulus in many cases. (Detailed discussions will be given in Secs. III A and III D). In the following, we will show that the observed trend in Fig. 1 can be correctly reproduced by the electronic structure calculations. It will be pointed out that the characteristic solid-solution hardening or softening is closely correlated with the change in the lattice constant. Very interestingly, the lattice constant of the Al-Li alloy varies nonmonotonically. We will demonstrate that the variation of the lattice constant with alloying is well accounted for by the first-order perturbation theory of the pseudopotentials. This implies that the lattice-constant variation has essentially nothing to do with the details of the band structures of the particular ordered compounds which we use in this study.

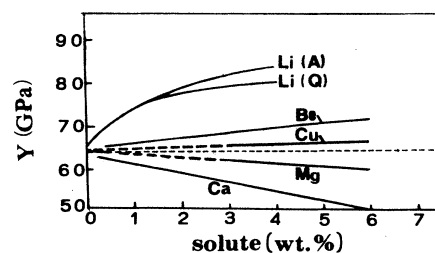


FIG. 1. Observed Young's moduli for the dilute Al-based alloys. For Li as a solute, A and Q in the parentheses denote annealed and quenched, respectively.

As for Al-Li alloys, Podlucky *et al.*¹¹ performed detailed electronic structure analyses recently and, as a part of their results, showed a decrease of bulk modulus by the Li addition. They referred to the experimental work by Müller *et al.*,¹² which also claimed a bulk-modulus decrease. The present result is in contradiction with these results. We will point out some possible problems in the experiment of Müller *et al.*

The present paper is organized in the following way. In Sec. II we outline the method of the band-structure calculations and bulk-modulus calculations of the Al-based alloys. Calculated results on bulk moduli of the Al-based ordered alloys and related discussions on the solid-solution hardening and softening will be presented in Sec. III. Concluding remarks will be made in Sec. IV.

II. METHOD OF CALCULATIONS

In order to discuss the solid-solution hardening or softening of Al-based fcc alloys, we estimate the bulk modulus of the ordered compounds with Al_7X and Al_3X compositions from the total-energy calculations: Li, Be, Na, Mg, Ca, and Cu are chosen as the solute elements X . The crystal structures of Al_7X and Al_3X ($L1_2$ structure) compounds, with 12.5 and 25 at. % solute concentrations, are shown in Figs. 2(a) and 2(b), respectively.

Although the crystal structure of Al_7X compound is rare in nature, it is useful to simulate the dilute solid solution of Al-based fcc alloys. For this Al_7X compound, the nearest-neighbor distance between the solute atoms is $\sqrt{2}$ times larger than that between the host Al atoms. Al_3X compound with $L1_2$ structure is introduced in order to investigate the concentration dependence on the solid-solution hardening or softening of the Al-based alloys. The $L1_2$ structure is also chosen for the reason that in the dilute (≈ 4 wt. %) Al-Li alloys a certain amount of metastable Al_3Li compound (δ' phase, $L1_2$ structure) is precipitated by the normal heat treatment and a possibility has been pointed out that the $\delta'(\text{Al}_3\text{Li})$ phase contributes significantly to the solid-solution hardening of the alloys.^{3,7-10} As will be discussed later, our analysis indicates that such an effect of $\delta'(\text{Al}_3\text{Li})$ is not significant.

The electronic structure and the total energy of the Al-based alloys are calculated self-consistently with the augmented-spherical-wave (ASW) method¹³ within the local density approximation (LDA), in the density functional theory. The ASW's up to $l=2$ are included for Al and Cu, while for Li, Be, Na, Mg, and Ca we use only those up to $l=1$. The number of k points used for the k -space integration is 220 for Al_3X and 288 for Al_7X in the irreducible wedge of the first Brillouin zone. As a LDA, we use the interpolation scheme proposed by Moruzzi *et al.*¹⁴

The calculated total energies for Al_3X and $\text{Al}_{3.5}\text{X}_{0.5}$ compounds are fitted to the form¹⁵

$$E_T = (p/a)^{2n} - (q/a)^n + r, \quad (1)$$

where a represents the lattice constant as indicated in Fig. 2 and p , q , and r the fitting parameters. (Note that we expand or compress both systems keeping the basic

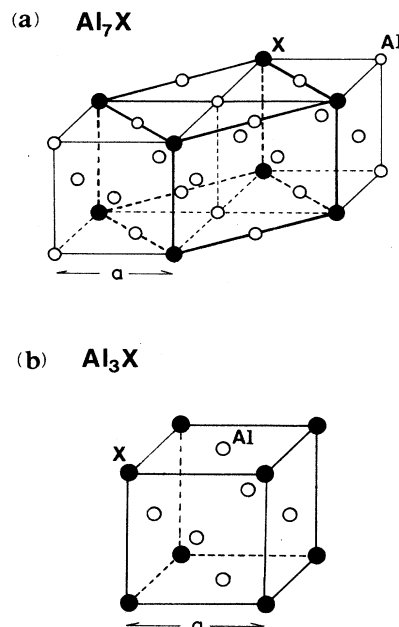


FIG. 2. The crystal structures adopted in the band calculations.

fcc lattice undistorted.) This type of fitting procedure works well for the Al-based Al_3X and Al_7X compounds with $n=3.5$ and enables us to get simple analytic expressions of the equilibrium lattice constants a_0 and the bulk modulus B of the alloys:

$$a_0 = 2^{1/n} p^2 / q, \quad (2)$$

$$B(a) = \frac{2np^{2n}}{9a^{2n+3}} \left[(2n+3) - (n+3) \left(\frac{a}{a_0} \right)^n \right]. \quad (3)$$

III. RESULTS AND DISCUSSIONS

A. Calculated bulk moduli

In the present study we restrict ourselves to the calculations of bulk moduli of Al-based alloys. However, one can generally draw definite conclusions on the solid-solution hardening or softening since bulk modulus B is related to other elastic constants in a simple manner. For instance, Young's modulus Y for cubic systems is given by¹⁶

$$Y = 3(1-2\nu)B, \quad (4)$$

where ν represents Poisson's ratio. Therefore, for materials with $\nu \approx \frac{1}{3}$, the magnitude of Young's modulus is almost identical to that of the bulk modulus.¹⁷

As mentioned before, the bulk modulus can be calculated quite straightforwardly from the total energy of the systems by using Eqs. (1)–(3). The fitting parameters p , q , and r , calculated equilibrium lattice constants a_0 and heats of formation ΔE_f are listed in Table I. Here ΔE_f is

TABLE I. Fitting parameters p , q , and r , equilibrium lattice constant a_0 and heat of formation ΔE_f of Al_7X and Al_3X compounds. All quantities are in Rydberg atomic units.

	p	q	r	a_0	ΔE_f
Al_4	7.4512	8.9371	0.8704	7.530	0.0
$(Al_7Li)/2$	10.4681	12.6350	0.9300	7.476	-0.034
$(Al_7Be)/2$	10.3001	12.3490	0.8451	7.405	0.072
$(Al_7Na)/2$	10.7237	12.9201	0.8201	7.672	0.070
$(Al_7Mg)/2$	10.6148	12.6223	0.8365	7.694	0.022
$(Al_7Ca)/2$	11.1078	13.1110	0.7735	8.112	0.144
$(Al_7Cu)/2$	10.3551	12.3888	0.8742	7.461	-0.020
Al_3Li	7.4422	9.0949	1.0115	7.424	-0.036
Al_3Be	7.0923	8.4860	0.8401	7.226	0.064
Al_3Na	7.2111	8.1216	0.5708	7.805	0.056
Al_3Mg	7.5437	8.8690	0.2745	7.822	0.026
Al_3Ca	7.9033	8.7481	0.5020	8.704	0.103
Al_3Cu	7.4054	9.1033	0.9887	7.344	-0.019

defined by

$$\Delta E_f\{Al_mX_n\} = E\{Al_mX_n; a_0\} - mE\{Al\} - nE\{X\}, \quad (5)$$

where $E\{Al_mX_n; a_0\}$ is the total energy of Al_mX_n at its equilibrium lattice constant and $E\{Al\}$ and $E\{X\}$ are the total energies of pure metals of Al and X with an assumption of a fcc lattice for X. One can see in Table I that the calculated lattice constants and heats of formation of Al-based alloys depend sensitively on the species of solute atoms. In general, solute elements which lead to incremental (decremental) lattice constants tend to decrease (increase) the elastic modulus of the alloys. The lattice-constant change will be discussed later in more detail by using a simplified pseudopotential theory.

In Fig. 3 we present the calculated bulk moduli of Al_7X

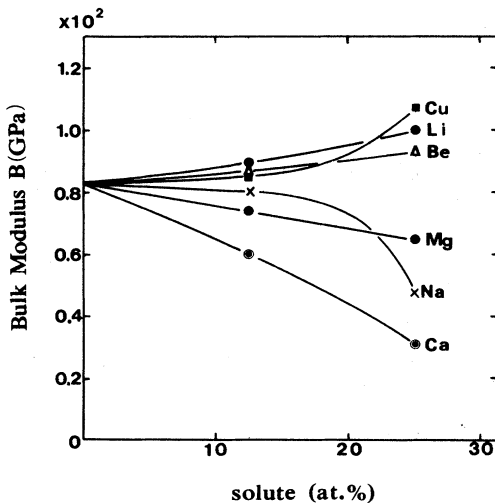


FIG. 3. Calculated bulk moduli vs solute concentration in at. %. Data points at 12.5 and 25 at. % are the actual results and the lines connecting them are simply a guide for the eye.

and Al_3X compounds. In the solute concentration range of less than 25 at. %, the bulk moduli of Al-based alloys depend almost linearly on the solute concentration, except for Al-Na and Al-Cu alloys. A slight upturn of B for the Al-Li alloy with respect to the Li concentration is qualitatively consistent with the enhancement in Young's modulus by annealing, which causes precipitation of $\delta'(Al_3Li)$. However, such an effect is of secondary importance in the solid-solution hardening for Al-Li alloys. In the Al-Cu or Al-Na systems, the bulk moduli increase or decrease nonlinearly and show marked changes at high solute concentrations. This may indicate that solute-solute interactions play an important role in determining the elastic moduli of these Al-based alloys.

In order to facilitate the comparison of the calculated bulk moduli B with the experimental elastic constants (Young's moduli in wt. %), we also present in Fig. 4 the calculated bulk moduli B against the solute concentration in wt. %. Comparing the elastic moduli of Al-based alloys presented in Figs. 1 and 4, one can see that there are good correlations between the calculated bulk moduli and experimental Young's moduli.

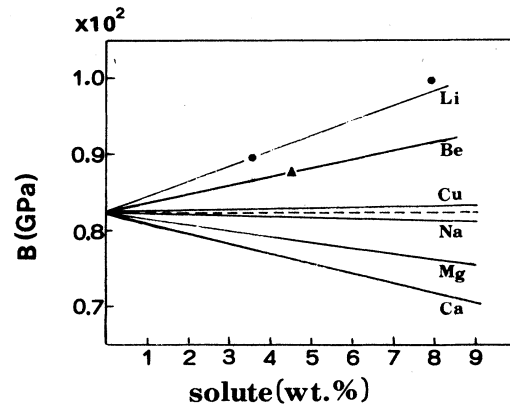


FIG. 4. Calculated bulk moduli vs solute concentration in wt. %. Lines connect the pure Al value with the data for 12.5 at. %.

B. Lattice-constant change

As mentioned in the preceding section, there seems to be a close correlation between the bulk-modulus change and the lattice-constant change. Therefore, as the first step toward the understanding of the solid-solution hardening or softening, we discuss the physical origin of the characteristic lattice-constant variation of Al-based alloys by adopting the first-order perturbation treatment of the electron-ion pseudopotential.¹⁸ Within this scheme based on the empty core model,¹⁹ the electron-sphere radius R_s of A - X alloy can be obtained by solving the following equations:¹⁸

$$\bar{R}_s^2 - 1 = c_A d_A (\bar{R}_{sA}^2 - 1) + c_X d_X (\bar{R}_{sX}^2 - 1), \quad (6)$$

with

$$\bar{R}_s = -1 + 0.452 R_s \left[0.916 + 1.8 \frac{c_A z_A^{5/3} + c_X z_X^{5/3}}{z} \right], \quad (7)$$

$$\bar{R}_{si} = -1 + 0.452 R_{si} (0.916 + 1.8 z_i^{2/3}), \quad (8)$$

and

$$d_i = \frac{z_i}{z} \frac{0.916 + 1.8(c_A z_A^{5/3} + c_X z_X^{5/3})/z}{0.916 + 1.8 z_i^{2/3}}, \quad (9)$$

where z_i ($i = A$ or X) is the valence number of A or X metal, c_i the concentration, z the average valence number given by $c_A z_A + c_X z_X$, R_s the electron-sphere radius of the A - X alloy, and R_{si} the equilibrium R_s value of the pure constituent. The electron-sphere radius R_s is defined as

$$R_s = \left[\frac{3}{4\pi n} \right]^{1/3} / a_H, \quad (10a)$$

with n being the valence electron density and a_H the Bohr radius, or

$$R_s = \left[\frac{3}{16\pi z} \right]^{1/3} \frac{a}{a_H}, \quad (10b)$$

in terms of the lattice constant a of a fcc lattice.

In order to discuss the lattice constants of dilute alloys (X being solute), we now expand the electron-sphere radius R_s and lattice constant a in terms of the solute concentration c_X . After some manipulations, we obtain

$$R_s \cong R_{sA} (1 + c_X P_2), \quad (11)$$

$$\begin{aligned} a &\cong a_A \left[1 - \frac{1}{3} c_X \frac{z_A - z_X}{z_A} \right] \frac{R_s}{R_{sA}} \\ &= a_A [1 + c_X (P_1 + P_2)], \end{aligned} \quad (12)$$

with

$$P_1 = -\frac{z_A - z_X}{3z_A}, \quad (13)$$

$$P_2 = \frac{R_{sX} - R_{sA}}{R_{sA}} \frac{z_X}{z_A} \frac{1}{\bar{R}_{sA}} \left[\frac{R_{sA} + R_{sX}}{2R_{sX}} (\bar{R}_{sX} + 1) - 1 \right], \quad (14)$$

with a_A the lattice constant of pure A metal. For alloy systems with $(R_{sA} - R_{sX})/2R_{sX} \ll 1$, Eq. (14) is reduced to

$$P_2 \cong \frac{R_{sX} - R_{sA}}{R_{sA}} \frac{B_X}{B_A}, \quad (15)$$

where B_i denotes the bulk modulus of pure i metal given by

$$B_i = \frac{4.42}{12} z_i \bar{R}_{si} / R_{si}^5. \quad (16)$$

Equations (11)–(15) provide us with a simple interpretation of the lattice-constant change in the dilute A - X alloy. Equations (11) and (15) state that the mean electron-sphere radius R_s deviates from a simple linear interpolation of R_{sA} and R_{sX} due to the difference in the bulk moduli between the pure A and X metals. If the metal X is much softer than the pure metal A ($B_A \ll B_X$), R_s hardly changes irrespective of the difference between R_{sA} and R_{sX} . In addition to the change in R_s , the valence electron number changes also in alloys. P_1 takes care of this contribution to the lattice constant.

In Fig. 5, we present the calculated lattice constants a as a function of solute concentration c_X . (In these figures, all the pure metals X are assumed to have a fcc structure and their lattice constants are estimated from their atomic density.) The lattice constants calculated by using the first-order pseudopotential theory are denoted by solid curves, while those obtained from the LDA-ASW calculation are denoted by solid circles. [The experimental lattice constant of Al_3Li is denoted by \times in Fig. 5(a). Also in the same figure, the open circles denote the calculated results by a modified method, as discussed in Sec. III D.] The dashed lines were obtained by linear extrapolation from the dilute limit. As we used experimental values for R_{si} (i.e., the lattice constant) in the pseudopotential calculations, we can judge the accuracy of the present LDA-ASW calculation at the pure metal limits.

We note large deviations from Vegard's law for the alkali-metal solutes, Li and Na, and in particular the non-monotonic variation of the lattice constant of the Al-Li alloy. The addition of Li to Al causes a shrinkage of the lattice for $c_{\text{Li}} < 0.86$, though the atomic volume of pure Li metal is larger than that of pure Al. (Note, however, that the Al-Li fcc phase is stable only to about 5 at. % of Li at room temperatures.) This is in fact observed experimentally and was reproduced also by Podloucky *et al.*,¹¹ although some significant discrepancy exists in quantitative aspects, which we will argue in detail in Sec. III D.

As mentioned above, Eqs. (11)–(15) provide us with useful information about the slope of the lattice-constant change in the dilute solution limit. For alkali-metal solutes with $z_X = 1$, P_1 makes a significant negative contribution of $-\frac{2}{9} = -0.222$. In addition to this, the bulk modulus of alkali metals is an order of magnitude smaller than that of Al and thereby P_2 is also reduced. The actual values of P_2 are 0.127 for Li and 0.250 for Na. Therefore the slope is negative for Li and slightly positive for Na. The larger P_2 for Na than for Li comes from the

difference in R_{sX} . We think that the lattice-constant decrease is the dominant source of the bulk-modulus enhancement in the Al-Li alloy.

For divalent solute elements ($z_X=2$), Be, Mg, and Ca, the deviation from Vegard's law is relatively small. Among them, Be causes a lattice-constant decrease as is shown in Fig. 5(b), which is correlated with the bulk-modulus enhancement. However, in contrast to the Al-Li case, the lattice-constant decrease in the Al-Be case seems to be nothing but a result of a small atomic volume of pure Be metal.

For Cu, it is well known that a simple pseudopotential theory does not work and the broken curve in Fig. 5(f)

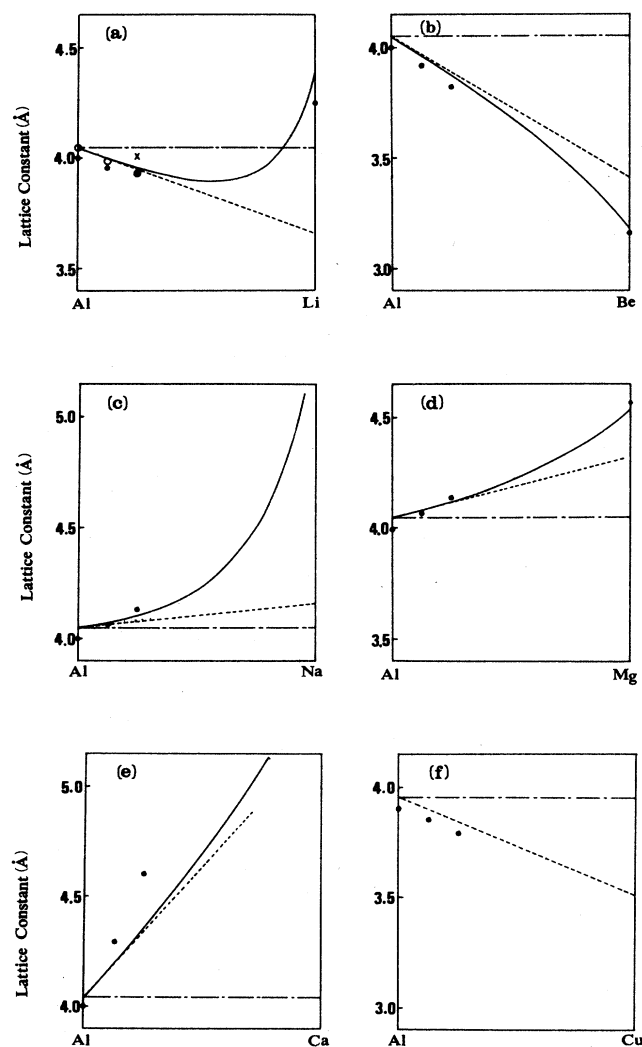


FIG. 5. Lattice-constant variations for the Al- X alloys with X being (a) Li, (b) Be, (c) Na, (d) Mg, (e) Ca, and (f) Cu. Solid circles denote the results of the ASW band calculations and solid curves those of the first-order perturbation theory of pseudopotentials. The dashed lines denote the initial slope estimated by Eq. (12). The cross in (a) is the experimental lattice constant of the precipitated δ' (Al₃Li) from Ref. 23. The open circles in (a) denote the results of the modified calculations as explained in Sec. III D.

denotes a linear interpolation of the two end metals, which is quite parallel with the results from the LDA-ASW calculations.

So far, we have shown that the lattice-constant change by alloying can be well reproduced by the first-order perturbation theory with the empty core model (except for the Al-Cu case) and that the lattice-constant decrease (increase) is correlated with the bulk-modulus enhancement (reduction) without any exception for those systems we are concerned with. This is a very important aspect not only because the first-order perturbation theory provides us with simple pictures of the problem but also because the success of the first-order perturbation implies that the details of the band structures and also the choice of the particular ordered compounds (Fig. 2) have little effect on the essential points of the present problems.

C. Effect of charge transfer to bulk moduli

It should be noted that although the first-order pseudopotential theory may give reasonable results for the equilibrium lattice constant, it is not accurate enough to discuss the bulk modulus.¹⁸ This is because the former quantity is related to the first derivative of the total energy with respect to volume while the latter is related to its second derivative which requires higher accuracy in the total-energy calculations. There are some subtle aspects in the bulk moduli quantitatively. For further discussions, we show in Fig. 6 the calculated bulk moduli for Al₇X, B_X , versus the corresponding equilibrium lattice

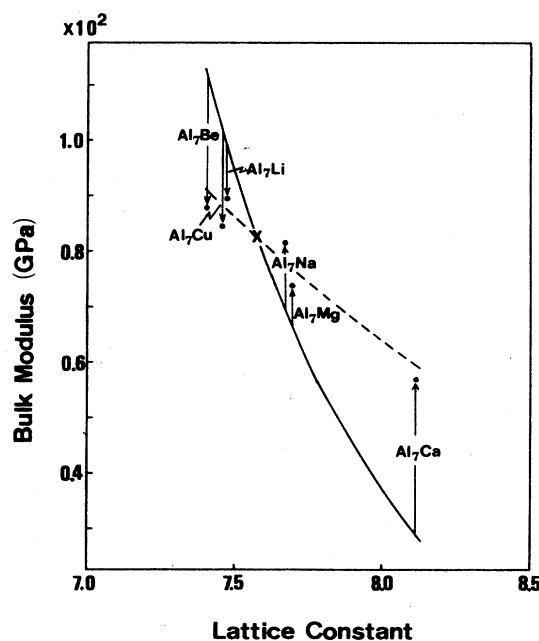


FIG. 6. The solid circles denote the calculated bulk moduli vs the equilibrium lattice constants for Al₇X. The solid curve is the lattice-constant dependence of the bulk modulus of pure Al estimated by Eq. (3). The cross denotes the calculated bulk modulus of Al at its equilibrium lattice constant. The dashed curve suggests a qualitative trend of B_X versus a_X .

constant, a_X , together with the lattice-constant dependence of the bulk modulus of the pure Al metal, $B_{Al}(a)$. An important observation is that although a nonmonotonic behavior of B_X as a function of a_X is seen for Be, Cu, and Li as X , the data seem to crudely follow the dashed curve whose slope is significantly reduced from that of $B_{Al}(a)$. The following qualitative analysis may help to explain this behavior.

We consider the internal pressure associated with each atomic sphere, and assume the same atomic sphere size between Al and X . We express the pressure for the Al atomic sphere in Al- X alloy as

$$P = P_{Al}(V, n), \quad (17)$$

where V is the atomic sphere volume and n is the valence electron number within the atomic sphere. When we change the volume of the whole system, the atomic sphere volume changes in the same ratio and n is adjusted so that the pressure at the Al site is the same as that at the X site.²⁰ Generally, n deviates from the pure Al value \bar{n} (\bar{n} being independent of volume) and we expand P to the first order with respect to $\Delta n = n - \bar{n}$:

$$P = P_{Al}(V, \bar{n}) + \Delta n \frac{\partial P_{Al}}{\partial n}. \quad (18)$$

The bulk modulus is given by

$$B = -V \frac{\partial P}{\partial V} \quad (19)$$

$$= -V \frac{\partial P_{Al}(V, \bar{n})}{\partial V} - V \frac{\partial \Delta n}{\partial V} \frac{\partial P_{Al}}{\partial n} - V \Delta n \frac{\partial^2 P_{Al}}{\partial V \partial n}. \quad (20)$$

The first term is approximately equal to the bulk modulus of pure Al for a given volume V (the solid line in Fig. 6) and the second and third terms give rise to modifications to it depending on the solute element X through Δn and $\partial \Delta n / \partial V$. In the latter two terms, $\partial P_{Al} / \partial n > 0$ and $(\partial^2 P_{Al} / \partial V \partial n) < 0$ may be reasonable, because the kinetic energy change may be more significant than the potential-energy change at the equilibrium volume. Furthermore, as Fig. 7 shows, Δn , the electron transfer from X to Al, is positive (negative) for X with a_X larger (smaller) than a_{Al} except in the case of Na. The sign of $\partial \Delta n / \partial V$ is opposite to that of Δn . (Mg is an exception in this respect.) These trends which are satisfied in most cases are physically meaningful: if Al is compressed in the Al- X alloy ($a_X < a_{Al}$), the valence electrons will flow out of the atomic sphere of Al in order to reduce the repulsive force due to the kinetic energy, so that $\Delta n < 0$; in such a situation, an increase in the repulsive force by compression will be more significant at Al than at X , leading to a further electron transfer from Al to X by a volume reduction, i.e., $\partial \Delta n / \partial V > 0$. Therefore both the second and third terms are positive for $a_X > a_{Al}$ and negative for $a_X < a_{Al}$ and thereby contribute to the reduction of the slope of B with respect to a .

The above argument is only approximate²⁰ and there

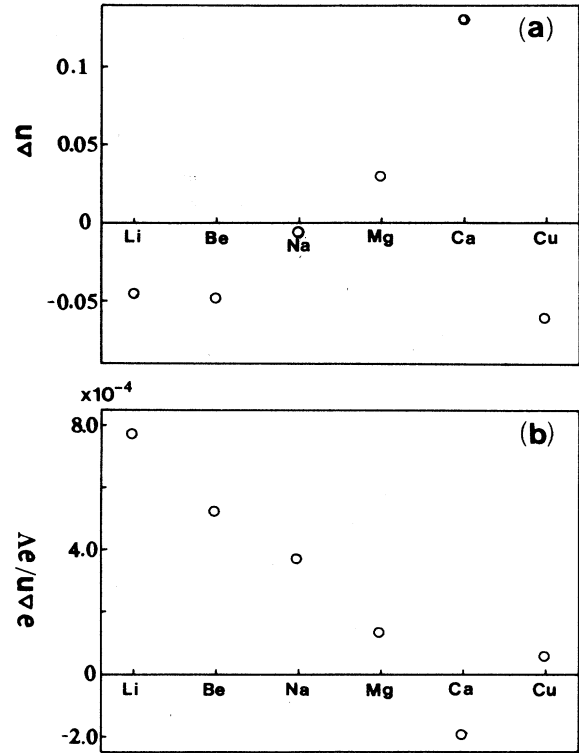


FIG. 7. (a) Δn denotes the change in the number of electrons in the atomic sphere of Al in the Al₇X systems with X being from Li to Cu. (b) The volume derivative of Δn . The values in (b) are in a.u.

are in fact some exceptions (Na and Mg). Nevertheless, it provides us with some hints about the relaxation effect due to the charge transfer between inequivalent sites associated with the volume change, which is absent in pure metals and may cause the reduction in slope of the dashed curve compared with the solid one in Fig. 6.

D. Problems in experimental and computational situations for Al-Li alloys

It is now well known that the Li deficiency extends up to 0.3 mm deep into the bulk from the surface in Al-Li alloys.²¹ Therefore experiments affected by this Li-deficient region will not provide us with reliable data for a given bulk concentration of Li. The lattice-constant measurement requires a caution. For example, a vanishingly small lattice parameter shrinkage (only by $\cong 0.1\%$) was reported for the Al-Li alloy with 21.53 at. % Li in 1963,²² while the recent review²³ cited 4.01 Å as the lattice constant of Al₃Li, which is reduced by 1% from that of pure Al. In the present calculation, the corresponding value is 1.5%, indicating a reasonable agreement but a slight overestimation of the lattice-constant shrinkage.

The experimental determination of the bulk modulus of the Al-Li alloy is also problematic. Müller *et al.*¹² measured three elastic constants by measuring the velocity of ultrasonic waves in three different modes and es-

estimated the Young's modulus Y and the bulk modulus B to conclude an enhancement in Y but a reduction in B by the Li addition. However, their increase in Y for the 4 at. % Li case with respect to the pure Al is only half of the corresponding value obtained by the direct measurement of Y by Noble *et al.*⁸ (The result of Noble *et al.* is consistent with other measurements.³) Independent measurement of Poisson's ratio ν of the Al-Li alloy is available: ν decreases slightly with increasing Li concentration, though some ambiguity exists quantitatively.²⁴ We estimated B by the Y values of Noble *et al.* and three possible variations for ν as shown in the inset of Fig. 8, which cover the ambiguous range in ν . In all three cases for ν , the bulk modulus is in fact enhanced in the Al-Li alloy (Fig. 8). On the other hand, if we use the estimation of Müller *et al.* for the increment in Y ,¹² the same procedure results in a reduction of the bulk modulus. We would like to point out also that the Debye temperature is enhanced by the Li addition to the Al metal.²⁵

As for the computational aspects, the local density approximation in the density functional theory is an approximation and the electronic structure calculation based on it tends to underestimate the lattice constant. In the present calculation, the lattice constant of fcc Al and bcc Li are underestimated by 1% and 3.5%, respectively. This results in an overestimation of bulk moduli: theoretical values are 82.3 GPa for Al and 18.4 GPa for Li, while experimental ones are 72.2 GPa for Al and 11.6 GPa for Li.²⁶ One may suspect that these discrepancies may seriously affect the lattice-constant change and the elastic-modulus enhancement in the Al-Li alloys, leading us to qualitatively wrong results. We therefore performed the following check calculations.

Considering that the LDA is in any case an approximation, we scaled the exchange-correlation potential and energy by a constant α as in the $X\alpha$ method.²⁷ α 's for Al and Li were adjusted so that the pure metal lattice constants could be correctly reproduced. This gives us $\alpha_{\text{Al}}=0.97$ and $\alpha_{\text{Li}}=0.91$. The resultant bulk moduli are 75.5 GPa for Al and 10.9 GPa for Li, in good agreement with experimental values. In the band-structure calculations for Al_7Li and Al_3Li , the same scaling factors α_{Al} and α_{Li} were used in the atomic spheres of Al and Li, respectively. The calculated lattice constants are shown in Fig. 5(a) by open circles. The rate of the lattice-constant shrinkage caused by the Li addition is rather enhanced in the new calculation compared with the results shown by solid circles. For example, the lattice-constant shrinkage of Al_3Li is now about 3%. This is not so strange, because both Al and particularly Li are much softer in the present calculation than in the previous one. Although the calculated lattice shrinkage looks too large compared with the experimental value, it should not be discarded. The lattice constant of Al_3Li is measured for the precipitated δ' phase surrounded by the α matrix whose lattice constant is larger than that of $\delta'(\text{Al}_3\text{Li})$.²³ It is therefore probable that the precipitated δ' phase may be exerted by a negative pressure to expand the lattice and that Al_3Li , if isolated, may have a smaller lattice constant than the observed one.

The bulk modulus B of Al_7Li in the new calculation is

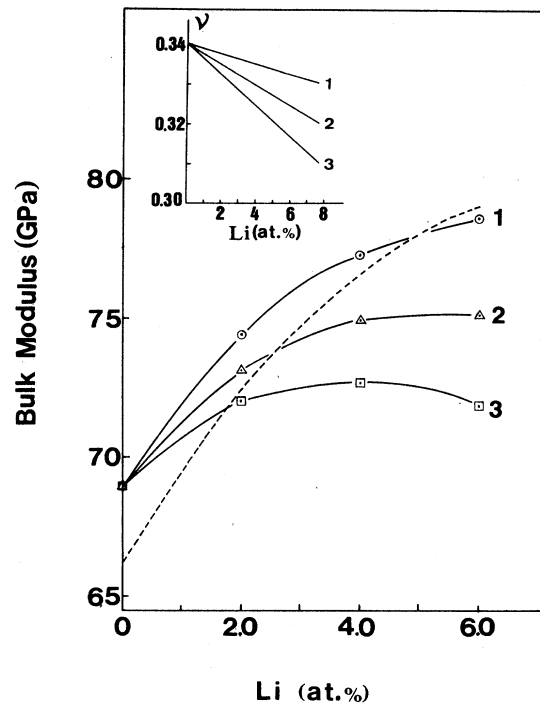


FIG. 8. The dashed curve denotes the observed Young's modulus vs the Li concentration (Ref. 8). The inset shows three possible variations for Poisson's ratio of the Al-Li alloys (Ref. 24). By combining Young's modulus with Poisson's ratio by Eq. (4), the bulk modulus was estimated as denoted by the three curves with the numbering corresponding to that for Poisson's ratio.

78.5 GPa, still larger than that of pure Al (75.5 GPa), but the enhancement is suppressed. On the other hand, B of Al_3Li is estimated to be 95.7 GPa being considerably enhanced, which may be correlated with the large lattice-constant shrinkage.

Summarizing the arguments in this subsection, we conclude that although there are some complications and ambiguities, it seems to be more probable that the bulk modulus of the Al-Li alloys is enhanced by the Li addition.

IV. CONCLUDING REMARKS

We have analyzed the microscopic origin of the solid-solution hardening and softening of the Al- X alloys with the solute X being Li, Be, Na, Mg, Ca, and Cu by performing the total-energy calculations based on the LDA for the ordered Al_7X and Al_3X compounds. The calculated bulk modulus for the Al- X system correlates very well with the observed Young's modulus. We have found that the solute which causes a lattice-constant decrease (increase) enhanced (reduces) the bulk modulus. It has been demonstrated that the lattice-constant change of the Al- X alloy (except for Cu as X) can be fairly well reproduced

by the first-order perturbation of the pseudopotential theory with the empty core model and a simple analytic expression has been derived for the initial slope of the lattice-constant change in the dilute limit of X . Qualitative discussions on the effect of charge transfer on the alloy bulk modulus have also been given.

Not only from technological interest but also from fundamental theoretical interest, detailed discussions have been given, particularly on the Al-Li alloys. The present analysis suggests that the initial decrease of the lattice constant by the Li addition, despite the larger atomic volume of Li than that of Al, is the main source of the enhancement in the bulk modulus (and Young's modulus also). Because of some complications and ambiguities both in experimental and theoretical situations, we have performed careful analyses on our calculated results to conclude that they should qualitatively be correct.

ACKNOWLEDGMENTS

The authors are grateful to Dr. Y. Miyagi and Dr. T. Etoh of Maoka Laboratory of Kobe Steel, Ltd. (Research Section, Maoka) for valuable discussions on solid-solution hardening of Al-based alloys. One of the authors (K.M.J.) is grateful also to the Visiting Researcher's Program of the Institute for Solid State Physics, under which this work was carried out. The original version of the ASW program package was coded by Dr. A. R. Williams, Dr. V. L. Moruzzi, and Professor J. Kübler, to whom the authors would like to express their sincere thanks. The numerical computations were carried out at the Computer Centers of the Institute for Solid State Physics and the Institute for Molecular Science.

*BITNET address: J40T@JPNISSP.

¹L. F. Modolfo, *Aluminum Alloys: Structure and Properties* (Butterworths, London, 1976).

²M. Tamura, T. Mori, and T. Nakamura, *Trans. Jpn. Inst. Metals* **14**, 355 (1973).

³D. Webster, in *Aluminum-Lithium Alloys*, edited by T. H. Sanders and E. A. Starke (AIME, New York, 1981), p. 228.

⁴T. H. Sanders, Jr. and E. A. Starke, Jr., *Acta Metall.* **30**, 927 (1982).

⁵S. Suresh, A. K. Vasudevan, M. Tosten, and P. R. Howell, *Acta Metall.* **35**, 25 (1987).

⁶K. A. Gschneidner, Jr., in *Solid State Physics*, edited by F. Seitz and D. Turnbull (Academic, New York, 1964), Vol. 16, p. 281.

⁷Y. Miyagi and T. Etoh, *Ind. Rare Metals (in Japanese)* **88**, 27 (1985).

⁸B. Noble, S. J. Harris, and K. Dinsdale, *J. Mater. Sci.* **17**, 461 (1982).

⁹K. R. Van Horn, *Aluminum* (American Society for Metals, Metals Park, Ohio, 1967).

¹⁰M. Furukawa, Y. Miura, and M. Nemoto, *Bull. Jpn. Inst. Metals (in Japanese)* **23**, 172 (1984).

¹¹R. Podloucky, H. J. F. Jansen, X. Q. Guo, and A. J. Freeman, *Phys. Rev. B* **37**, 5478 (1988).

¹²W. Müller, E. Bubeck, and V. Gerald, in *Aluminum-Lithium Alloys III*, edited by C. Baker, P. J. Gregson, S. J. Harris, and C. J. Peel (Institute of Metals, London, 1986), p. 435.

¹³A. R. Williams, J. Kübler, and C. D. Gelatt, Jr., *Phys. Rev. B* **19**, 6094 (1979).

¹⁴V. L. Moruzzi, J. F. Janak, and A. R. Williams, *Calculated*

Properties of Metals (Pergamon, New York, 1978).

¹⁵K. Terakura, T. Oguchi, T. Mohri, and K. Watanabe, *Phys. Rev. B* **35**, 2169 (1987).

¹⁶J. P. Hirth and J. Lothe, *Theory of Dislocations* (Wiley, New York, 1982).

¹⁷For Al-Li alloys, an appreciable variation of ν with regard to the Li concentration makes the argument complicated to some extent. More details about the experimental situation are given in Sec. III D.

¹⁸J. Hafner, *From Hamiltonian to Phase Diagrams* (Springer-Verlag, Berlin, 1987).

¹⁹N. W. Ashcroft, *Phys. Lett.* **23**, 48 (1966).

²⁰This does not hold in a rigorous sense, because pressure is a macroscopic concept and Pascal's principle does not necessarily hold in the microscopic scale. In fact, we found that for Al₇Na the pressure associated with the Na atomic sphere is more positive than that for the Al atomic sphere with the same atomic radii for Na and Al.

²¹H. Ueda, A. Matui, M. Furukawa, Y. Miura, and M. Nemoto, *Trans. Jpn. Inst. Metals*, **49**, 562 (1985).

²²E. D. Levine and E. J. Papperport, *Trans. AIME* **227**, 1204 (1963).

²³E. J. Lavernia and N. J. Grant, *J. Mater. Sci.* **22**, 1521 (1987).

²⁴J. Grazer and J. W. Morris, Jr., *AIAA J.* **25**, 1271 (1987).

²⁵A. G. Fox and R. M. Fisher, *Acta Crystallogr., Sect. A* **43**, 260 (1987).

²⁶C. Kittel, *Introduction to Solid State Physics*, 6th ed. (Wiley, New York, 1986), p. 57.

²⁷J. C. Slater, *Quantum Theory of Molecules and Solids* (McGraw-Hill, New York, 1974), Vol. 4, Chap. 1.